THE EFFECTIVE THERMAL DIFFUSIVITY OF PACKED FLUIDIZED BEDS

A. I. Tamarin and R. R. Khasanov UDC 66.036.5

The effective thermal diffusivity has been examined for several types of small-volume packings; experimental results for two materials and all types of packing are presented as an empirical relationship.

Various heterogeneous technical processes can employ fluidized systems with a fixed packing [1], as the latter break up the gas bubbles and produce a bed of high homogeneity, though they simultaneously reduce the motion of solid [1, 2]. Therefore, considerable interest attaches to experimental evidence on the solid mixing in the system. Unfortunately, such data have been published only for certain types of packing. The data are more or less reliable for a fluidized bed with spherical packing (bed of large spheres) [3-5]. Fragmentary data have been published for several types of small-volume packings: set of horizontal grids [6, 7], a stack of grid cylinders [3], and wire spiral packings [2]. On the other hand, nothing has been published on the mixing of the solid in such a bed when the packing is in the form of a set of finned vertical tube bundles, or sets of packets of flat inclined plates, although these are of industrial interest.

We have remedied this deficiency and obtained information on the mixing rate (heat transfer in space) for such a fluidized bed.

The experiments were done in a column of diameter 300 mm, with air fluidizing sand ($d = 0.23$ mm, $U_0 = 6$ cm/sec) and silica gel ($d = 0.19$ mm, $U_0 = 2$ cm/sec). We used several types of packing, whose major characteristics are given in Table 1. The tests were done with initial bed heights of 30, 45, and 60 cm and fluidization numbers up to 20.

The heat transfer rate in the vertical direction was determined with an instantaneous thermal pulse [7]. A bunch of hot particles was produced by a heat source at the upper boundary of the layer, and the time needed for the temperature to begin to rise at the lower boundary, τ_m, was measured. This gave the effective thermal diffusivity [7] as

$$a_{\text{eff}} = \frac{L^2}{2\tau_m}. \tag{1}$$

The value is dependent on the gas flow rate U, layer height H_0; and the aerodynamic characteristic of the material U_0. These quantities can be grouped as two dimensionless combinations a_{eff}/U_0H_0 and $U/U_0 = N$.

Figure 1 shows the observed relation between the effective thermal diffusivity and the gas-passage speed in terms of these dimensionless coordinates. The points are shown for sand and silica gel. We give not only values for a free fluidized layer but also ones with packings Nos. 3 and 4 (Table 1), and it is clear that the observed points for the free layer lie appreciably higher than those for ones with packing, which indicates that the immobile packing reduces the mixing rate.

The points for the free layer lie around one straight line, while those for packings Nos. 3 and 4 lie around others. Each of the straight lines passes near the origin, but the slopes differ. The same applies for the other types of packing.

Institute of Heat and Mass Transfer, Academy of Sciences of the Belorussian SSR, Minsk. Translated from Inzhenerno-Fizicheskii Zhurnal, Vol. 27, No. 3, pp. 491-496, September 1974. Original article submitted November 12, 1973.

TABLE 1. Packing Characteristics

Group	No.	Parameters, etc	Hydraulic diameter 1H, cm	Char. size, mm	Notes
I	1	Free layer	—	—	
II		Low-volume packing		Pitch of set	H=0,46 cm
	2	Set of vertical tubes ϕ 20 mm	8,06	63×63	
	3	Wire spirals D = 55 mm [8]	3,0	Packed loosely	
	4	Wire spirals, D = 20 mm	0,52	Packed loosely	
	5	Wire spirals, D = 10 mm	0,34	Packed loosely	
	6	Set of vertical tubes ϕ 20 mm With three straight longitudinal edges in each	2,7	63×63	Edge width 20 mm, thickness 2 mm
	7	Set of vertical tubes ϕ 20 mm with one start spiral edge, pitch S = 132 mm	4,35	63×63	"
	8	Set of vertical tubes ϕ 20 mm With two-start spiral edge, pitch S = 132 mm	2,86	63×63	Edge width 20 mm, thickness 2 mm
	9	Set of vertical tubes ϕ 20 mm With one start spiral edge; pitch S = 222 mm	4,54	63×63	"
	10	Set of vertical tubes ϕ 20 mm with two-start spiral edge, pitch S = 222 mm	3,22	63×63	"
III		Plate packing		Slot width, mm	H=1.45 cm
	11	Vertical plates in pack, height h = 55 mm, pitch S = 50 mm, thickness 1 mm, inclination to horizontal α = 90°	2,04	50	
	12	Plates in a pack, neighbors all inclined in the same direction, h = 55 mm, S = 50 mm, α = 60°	1,92	50	
	13	Plates in a pack, neighbors inclined in opposite directions, h = 55 mm, S = 34 mm, α = 75°	1,59	18	
	14	As 13, h = 35 mm, S = 20 mm, α = 75°	1,14	12	"
	15	Layer of spheres			H=0.64 cm

The immobile elements present additional obstacles to circulation; the projection of the particle velocity normal to the surface is zero, so the packing may be characterized to a first approximation via its hydraulic radius (l, H), i.e., the volume of the fluidized bed per unit packing surface.

Figure 2 shows in semilog terms the relation of a_{eff} to the hydraulic radius for afixed fluidization number N = 11; it shows experimental results for all our packings, and also data for a spherical packing (layer of large spheres) published elsewhere [3, 4].

The points all lie around three straight lines. The top one represents small-volume packings Nos. 2-10 (bundles of finned tubes and layers of wire spirals), while the second represents a layer of large spheres, and the third (lower) straight line represents packets of plates (Nos. 11-14). All these straight lines run through the point corresponding to mixing of the solid in a free fluidized bed, but they differ in slope H = $(1/U_0H_0)(\partial a_{eff}/\partial 1/l_H)$ and the latter is essentially a characteristic of the packing construction and reflects the differences in effect from the different parts of the surface of the immobile element. We can say that the plate packs are most effective, with the low-volume packings (finned tubes and wire spirals) least effective. The sphere packing is intermediate. The values of H, the design parameter of a packing group, are as follows: low-volume packings 2-10, plates 11-14, and a layer of spheres respectively H = 0.46; 0.15; and 0.64 (Table 1).

Figure 3 shows a final result from processing the data, and it represents our results with three beds and ones with packings Nos. 2-4 (Table 1) as well as other results for spherical packings [3, 4]. The following relationship applies approximately:

$$\frac{a_{eff}}{\nu_g} = \frac{120(N-2)}{1+\left(\frac{800}{\mathrm{Re}_*}\right)^2} \exp\left(-\frac{H}{l_H}\right), \quad (2)$$

where Re* $= U_0H_0/\nu_g$.

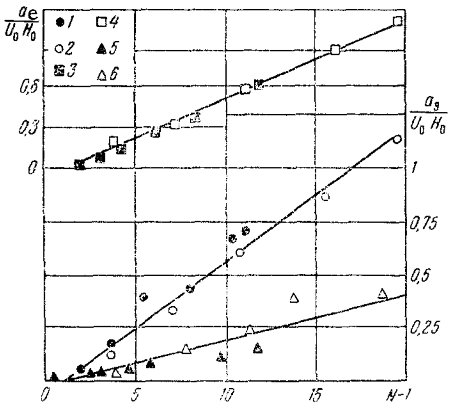

Fig. 1

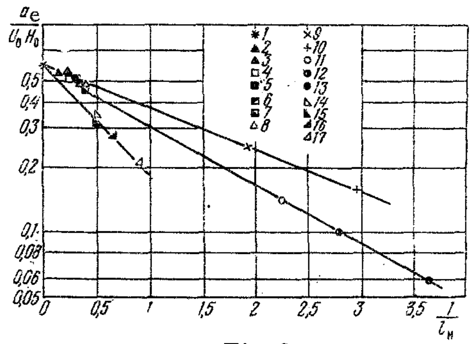

Fig. 2

Fig. 1. Effective thermal diffusivity as a function of gas passage rate: 1, 3, and 5) sand d = 0.23 mm with packings 1, 3, and 4 respectively (Table 1); 2, 4, and 6) silica gel, d = 0.19 mm, packings 1, 3, and 4 respectively (Table 1).

Fig. 2. Effective thermal diffusivity as a function of reciprocal hydraulic radius of packing ($1/l_H$, cm^{-1}): 1) free layer; 2-10) respectively packings 2, 9, 7, 10, 3. 6, 8, 4, and 5 (Table 1); 11) layer of spheres [3]; 12 and 13) layer of spheres [4]; 14-17) packings 11, 12, 13, and 14 respectively.

The values apply for $2 \leq N \leq 20$, $0.3 \leq l_H \leq 10$ cm, $1.5 \leq U_0 \leq 6$ cm/sec; $30 \leq H_0 \leq 60$ cm, $Re_* < 2500$; $\nu = 0.15$ cm^2/sec; the maximum spread in the observed points does not exceed 30%, which is quite acceptable for this system.

The result shows that the mixing rate increases linearly with the fluidization number but falls as the hydraulic radius of the packing increases. The particle circulation begins to make itself felt at fluidization numbers above 2. The linear relationship to the speed for onset of fluidization is also interesting. The height dependence is complex; if the height is small ($Re_* < 10^3$), the mixing rate increases rapidly, but with the rate of increase gradually falling. Above the value

$$Re_* = \frac{U_0 H_0}{\nu_g} \simeq 2000, \tag{3}$$

the circulation of the solid is virtually independent of the height. Equation (3) can be considered as an estimate for the vertical scale of the solid circulation loop in a fluidized bed with a packing. The layer height above which the mixing rate becomes constant varies inversely with the speed for onset of fluidization.

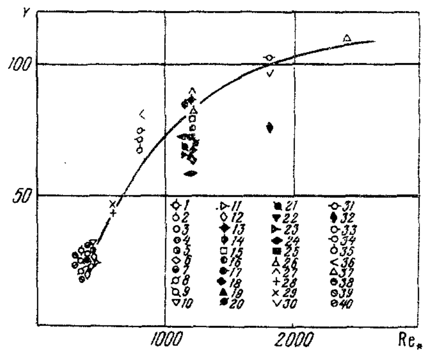

Fig. 3. Generalized curve. Dispersed material silica gel d = 0.19 mm, H_0 = 30 cm; 1-12) sand d = 0.23 mm, H_0 = 30 cm; 13-26) Nos. 1-14 (Table 1); silica gel H_0 = 45 cm; 28, 29) Nos. 3, 4 (Table 1); sand H_0 = 45 cm; 30, 31, 32) Nos. 3, 4, 12 (Table 1); silica gel H_0 = 60 cm; 33, 34, 35, 36) Nos. 3, 7, 9, 8 (Table 1); sand H_0 = 60 cm; 37) Nos. 4 (Table 1); 38) [3]; 39, 40) [4]; $Y = a_{eff} \exp(H/l_H)/(N-2)\nu_g$; $Re_* = U_0 H_0/\nu_g$.

The empirical relationships can be recommended in estimating the heat-transport rate in a fluidized bed with packing and also for evaluating the solid circulation. This information is necessary in constructing an approximate model for any process involving a fluidized bed with packing, especially if a sound choice of optimal parameters is necessary.

NOTATION

a_{eff}, effective thermal conductivity; L, distance from surface to thermocouple; τ_m time; U_0, U, fluidization onset velocity and interstitial gas velocity; H_0, height of packed layer; N, fluidization number; I_H, hydraulic radius of packing; ν_g, kinematic viscosity of gas; d, particle diameter; H, packing parameter.

LITERATURE CITED

1. J. R. Grace and D. Harrison, Chem. and Proc. Engng., No. 6, 127-130 (1970).
2. A. I. Tamarin, D. M. Galevshtein, S. S. Zabrodskii, R. R. Khasanov, and V. P. Borisenko, Inzh.-Fiz. Zh., 23, No. 4 (1971).
3. K. Kato, K. Imofuku, K. Hattori, and H. Kubota, Kagaku Kogaku (Chem. Eng. Japan), 5, No. 1, 66-69 (1967).
4. J. D. Gabor, "Axial solids mixing in fluidized packed beds," Chem. Eng. Progr. Sympos. Ser., 62, No. 67 (1966).
5. E. N. Ziegler and W. T. Braxelton, "Radial heat transfer in a packed fluidized bed," JEC Process Design Develop., 2, No. 4 (1963).
6. L. Massimilla and J. W. Westwater, A. J. Ch. E. Journal, 6, No. 1, 134-138 (1960).
7. V. A. Borodulya and A. I. Tamarin, Inzh.-Fiz. Zh., 5, No. 11 (1962).
8. A. I. Tamarin and V. D. Dunskii, Author's Certificate No. 242146, Byul. Izobr., No. 15 (1969).
9. S. S. Zabrodskii, A. I. Tamarin, and D. M. Galrshtein, Authors' Certificate No. 306867 Byul. Izobr., No. 20 (1971).